REPORT DOCUMENTATION PAGE

Form Approved
OMB No. 0704-0188

The public reporting burden for this collection of information is estimated to average 1 hour per response, including the time for reviewing instructions, searching existing data sources, gathering and maintaining the data needed, and completing and reviewing the collection of information. Send comments regarding this burden estimate or any other aspect of this collection of information, including suggestions for reducing the burden, to the Department of Defense, Executive Services and Communications Directorate (0704-0188). Respondents should be aware that notwithstanding any other provision of law, no person shall be subject to any penalty for failing to comply with a collection of information if it does not display a currently valid OMB control number.

PLEASE DO NOT RETURN YOUR FORM TO THE ABOVE ORGANIZATION.

1. REPORT DATE (DD-MM-YYYY)	2. REPORT TYPE	3. DATES COVERED (From - To)
13-01-2010	Journal Article	

4. TITLE AND SUBTITLE
Factors Contributing to Corrosion of Steel Pilings in Duluth-Superior Harbor

5a. CONTRACT NUMBER

5b. GRANT NUMBER

5c. PROGRAM ELEMENT NUMBER

6. AUTHOR(S)
Richard Ray, J. Lee, B. Little

5d. PROJECT NUMBER

5e. TASK NUMBER

5f. WORK UNIT NUMBER
73-9776-09-5

7. PERFORMING ORGANIZATION NAME(S) AND ADDRESS(ES)
Naval Research Laboratory
Oceanography Division
Stennis Space Center, MS 39529-5004

8. PERFORMING ORGANIZATION REPORT NUMBER
NRL/JA/7330-09-9285

9. SPONSORING/MONITORING AGENCY NAME(S) AND ADDRESS(ES)
Office of Naval Research
800 N. Quincy St.
Arlington, VA 22217-5660

10. SPONSOR/MONITOR'S ACRONYM(S)
ONR

11. SPONSOR/MONITOR'S REPORT NUMBER(S)

12. DISTRIBUTION/AVAILABILITY STATEMENT
Approved for public release, distribution is unlimited.

20100121313

13. SUPPLEMENTARY NOTES

14. ABSTRACT
Field observations and laboratory testing were used to conclude that aggressive localized corrosion of carbon steel pilings in Duluth-Superior Harbor, Minnesota and Wisconsin, is caused by the following sequence of biological, chemical, and physical events. Iron-oxidizing bacteria colonize the carbon steel sheet pilings and produce tubercles, made up of intact and/or partially degraded remains of bacterial cells mixed with amorphous hydrous ferric oxides. The reducing conditions beneath the tubercles cause copper dissolved in the water to precipitate. A galvanic couple is established between the copper layer and the iron substratum. Ice scouring breaks the tubercles. Exposure of the copper-covered iron to oxygen causes the galvanic current to increase. The result is aggressive localized corrosion.

15. SUBJECT TERMS
bacteria, carbon steel, corrosion, Duluth-Superior Harbor, microbiologically influenced corrosion, pilings

16. SECURITY CLASSIFICATION OF:			17. LIMITATION OF ABSTRACT	18. NUMBER OF PAGES	19a. NAME OF RESPONSIBLE PERSON
a. REPORT	b. ABSTRACT	c. THIS PAGE			Richard Ray
Unclassified	Unclassified	Unclassified	UL	11	19b. TELEPHONE NUMBER (Include area code) 228-688-4690

PUBLICATION OR PRESENTATION RELEASE REQUEST

Pubkey: 6219 NRLINST 5600.2

1. REFERENCES AND ENCLOSURES	2. TYPE OF PUBLICATION OR PRESENTATION		3. ADMINISTRATIVE INFORMATION
Ref: (a) NRL Instruction 5600.2 (b) NRL Instruction 5510.40D Encl: (1) Two copies of subject paper (or abstract)	( ) Abstract only, published ( ) Book ( ) Conference Proceedings (refereed) ( ) Invited speaker (X) Journal article (refereed) ( ) Oral Presentation, published ( ) Other, explain	( ) Abstract only, not published ( ) Book chapter ( ) Conference Proceedings (not refereed) ( ) Multimedia report ( ) Journal article (not refereed) ( ) Oral Presentation, not published	STRN NRL/JA/7330-09-9295 Route Sheet No. 7330/ Job Order No. 73-9776-09-5 Classification X U C Sponsor MISC DOD approval obtained yes X no

4. AUTHOR

Title of Paper or Presentation Factors contributing to corrosion of steel pilings

~~A Novel Mechanism for~~ Microbiologically Influenced Corrosion in Duluth-Superior Harbor

Author(s) Name(s) (*First,MI,Last*), *Code, Affiliation if not NRL*

Richard I. Ray, Jason S. Lee, Brenda J. Little

It is intended to offer this paper to the _____
(*Name of Conference*)

_____
(*Date, Place and Classification of Conference*)

and/or for publication in **Corrosion, Unclassified**
(*Name and Classification of Publication*) (*Name of Publisher*)

After presentation or publication, pertinent publication/presentation data will be entered in the publications data base, in accordance with reference (a).
It is the opinion of the author that the subject paper (is ____) (is not ___X) classified, in accordance with reference (b).
This paper does not violate any disclosure of trade secrets or suggestions of outside individuals or concerns which have been communicated to the Laboratory in confidence. This paper (does ____) (does not ___X) contain any militarily critical technology.
This subject paper (has ____) (has never _X_) been incorporated in an official NRL Report.

Richard I. Ray, 7332 Richard I Ray
Name and Code (*Principal Author*) (Signature)

5. ROUTING/APPROVAL

CODE	SIGNATURE	DATE	COMMENTS
Author(s) Ray	R Ray	7.01.09	Need by 24 Jul 09 Publicly accessible sources used for this publication
Section Head Brock Faugeo	Jeffrey W. Brock	7-2-09	acting
Branch Head **Robert A Arnone, 7330**	R W Gould	7/2/09	acting
Division Head **Ruth H. Preller, 7300**	Ruth H Preller	7/2/09	1. Release of this paper is approved. 2. To the best knowledge of this Division, the subject matter of this paper (has ____) (has never _X_) been classified.
Security, Code **1226**			1. Paper or abstract was released. 2. A copy is filed in this office. SSC 239-9
Office of Counsel,Code **1008.3**			
ADOR/Director NCST **E. R. Franchi, 7000**			
Public Affairs (*Unclassified/ Unlimited Only*), Code **7030.4**	Deborah Spratt	7/9/09	
Division, Code			
Author, Code			

PUBLICATION OR PRESENTATION RELEASE REQUEST 09-1226-2353

Pubkey: 219 NRLINST 5600.2

Ref: (a) NRL Instruction 5600.2
(b) NRL Instruction 5510.40D

Encl: (1) Two copies of subject paper (or abstract)

( ) Abstract only, published
( ) Book
( ) Conference Proceedings (refereed)
( ) Invited speaker
(X) Journal article (refereed)
( ) Oral Presentation, published
( ) Other, explain

( ) Abstract only, not published
( ) Book chapter
( ) Conference Proceedings (not refereed)
( ) Multimedia report
( ) Journal article (not refereed)
( ) Oral Presentation, not published

STRN NRL/JA/7330-09-9285
Route Sheet No. 7330/
Job Order No. 73-9776-09-5
Classification X U ___ C
Sponsor MISC DOD
approval obtained ___ yes X no

Title of Paper or Presentation Factors contributing to corrosion of steel pilings 80-5
~~A Novel Mechanism for Microbiologically Influenced Corrosion~~ in Duluth-Superior Harbor

Author(s) Name(s) (*First,MI,Last*), Code, Affiliation if not NRL

Richard I. Ray, Jason S. Lee, Brenda J. Little

It is intended to offer this paper to the _____
(*Name of Conference*)

_____
(*Date, Place and Classification of Conference*)

and/or for publication in Corrosion, Unclassified
(*Name and Classification of Publication*) (*Name of Publisher*)

After presentation or publication, pertinent publication/presentation data will be entered in the publications data base, in accordance with reference (a).
It is the opinion of the author that the subject paper (is ____) (is not X) classified, in accordance with reference (b).
This paper does not violate any disclosure of trade secrets or suggestions of outside individuals or concerns which have been communicated to the Laboratory in confidence. This paper (does ____) (does not X) contain any militarily critical technology.
This subject paper (has ____) (has never X) been incorporated in an official NRL Report.

Richard I. Ray, 7332 — Richard I Ray
Name and Code (*Principal Author*) (Signature)

CODE	SIGNATURE	DATE	COMMENTS
Author(s) Ray	R Ray	7.01.09	Need by 24 Jul 09
			Publicly accessible sources used for this publication
Section Head Book Teague		7-2-09	acting
Branch Head Robert A Arnone, 7330	RWGould	7/2/09	acting
Division Head Ruth H. Preller, 7300		7/2/09	1. Release of this paper is approved. 2. To the best knowledge of this Division, the subject matter of this paper (has ____) (has never X) been classified.
Security, Code 1226		7/6/09	1. Paper or abstract was released. 2. A copy is filed in this office. SSC 238-9
Office of Counsel, Code 1008.3			
ADOR/Director NCST E. R. Franchi, 7000			This is a Final Security Review. Any changes made in the document after approved by Code 1226 nullify the Security Review
Public Affairs (*Unclassified/ Unlimited Only*), Code 7030.4		7/7/09	
Division, Code			
Author, Code			JUL 6 PM 4:47

HQ-NRL 5511/6 (Rev. 12-98) (e) THIS FORM CANCELS AND SUPERSEDES ALL PREVIOUS VERSIONS

Factors Contributing to Corrosion of Steel Pilings in Duluth-Superior Harbor

R. Ray,* J. Lee,‡,* and B. Little*

ABSTRACT

Field observations and laboratory testing were used to conclude that aggressive localized corrosion of carbon steel pilings in Duluth-Superior Harbor, Minnesota and Wisconsin, is caused by the following sequence of biological, chemical, and physical events. Iron-oxidizing bacteria colonize the carbon steel sheet pilings and produce tubercles, made up of intact and/or partly degraded remains of bacterial cells mixed with amorphous hydrous ferric oxides. The reducing conditions beneath the tubercles cause copper dissolved in the water to precipitate. A galvanic couple is established between the copper layer and the iron substratum. Ice scouring breaks the tubercles. Exposure of the copper-covered iron to oxygen causes the galvanic current to increase. The result is aggressive localized corrosion.

KEY WORDS: bacteria, carbon steel, corrosion, Duluth-Superior Harbor, microbiologically influenced corrosion, pilings

INTRODUCTION

Carbon steel (CS) sheet piling (1.2-cm-thick A328[1] cold-rolled) used for docks, bridges, and bulkheads in the Duluth-Superior Harbor (DSH), Minnesota and Wisconsin, is corroding at an accelerated rate.[2-3] DSH is located at the extreme western end of Lake Superior and is described as a freshwater estuary.[4] The Lake Superior watershed has been described "as an ecosystem that was disturbed earlier by turn-of-the-century mining in a patchwork manner along the shoreline. Portions of the lake are in a recovery phase, whereas other areas are still impacted by slow resuspension-deposition dynamics and continuing mining activities."[5]

Of all the Great Lakes, Lake Superior contains the strongest development of a separate coastal regime, chemically and biologically distinct from offshore waters.[6] Kerfoot and Robbins[6] cite erosion of metal-rich ore bodies around Lake Superior as a source of Cu enrichment in shoreline sediments. Lake Superior is a monomictic lake, meaning that during the summer it separates into two layers based on water density, then from fall to spring the layers are mixed together causing a cycling of elements. DSH is polymitic, i.e., seiches or free standing wave oscillations are almost always present, suspending particulates into the water column.[7] DSH is icebound from mid-December to mid-April and during that time has a durable, well-defined ice cover.[4] Freeze ice thicknesses in DSH range from 0.5 m to 1.4 m in addition to snow ice, stack ice, and ice from wave and splash action along harbor walls.[8]

The corroded pilings (Figure 1[a]) have an orange rusty appearance characterized by tubercles. The term tubercle is used throughout this paper to describe corrosion products and deposits covering areas of localized corrosion. Divers report that tubercles are randomly distributed from the waterline to approximately 3 m below the surface.[8] Scott, et al.,[8] report that tubercles can be removed by hand and that regrowth occurs. Tubercles vary in diameter from a few millimeters to several centimeters and

Submitted for publication July 2009; in revised form, August 2009.

‡ Corresponding author. E-mail: jason.lee@nrlssc.navy.mil.
* Naval Research Laboratory, Code 7332, Stennis Space Center, MS 39529-5004.

ISSN 0010-9312 (print), 1938-159X (online)
09/000129/$5.00+$0.50/0 © 2009, NACE International

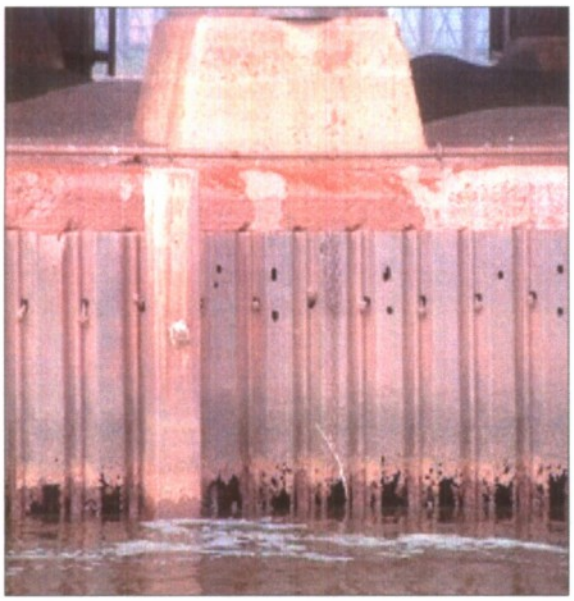

FIGURE 1. *DSH piling with visible perforation at the water line. Photograph reproduced with permission from Gene Clark, Wisconsin Sea Grant Program.*

TABLE 1
Corrosion and Water Quality
Water: Slightly Alkaline (pH 7.5 to 8.5), Oxic (7 to 9 mg O_2/L)

Site	Corrosion Rating[(A)]	Sulfate[(B)] (mg/L)	Chloride[(B)] (mg/L)
Duluth Entry	Low-Moderate	4 to 6	<10
Cutler-Magner	—	19	14
Midwest Energy	High	32	21
Oliver Bridge	Moderate	14	11
Superior Entry	Low-Moderate	6 to 16	10 to 1

[(A)] Characterization by AMI Consulting Engineers (Duluth, Minnesota).
[(B)] September 19-24, 2006; Trace Analytical Laboratories, Inc. (Muskegon, Michigan).

when removed, large and often deep pits are exposed. In some cases the CS is perforate. Below 3 m the attached zebra mussel (*Dressena polymorpha*) population is dense and few tubercles are observed. Zebra mussels are small, fingernail-sized mussels native to the Caspian Sea. They were first observed in Lake St. Clair, Minnesota, in 1988 and have since spread to all of the Great Lakes.

Accelerated corrosion of CS pilings in estuarine and marine harbors is a global phenomenon.[9] The term "accelerated low water corrosion" (ALWC) is used to identify the phenomenon. The detailed mechanism of ALWC in marine/estuarine environments continues to be a matter of some debate, but several researchers have concluded that it is a form of microbiologically influenced corrosion (MIC).[10,11] Gehrke and Sand[12] completed a three-year study of pilings in German marine harbors with and without corrosion. They concluded that the ALWC was due to a combination of sulfate-reducing bacteria (SRB) and thiobacilli in the fouling layers on the pilings. The sulfides produced by the SRB in the anaerobic regions and sulfuric acid resulting from the thiobacilli in the aerobic regions combined to produce an extremely corrosive environment.

There are obvious differences in the observations in DSH and reports of ALWC. ALWC is observed in the low water zone, just below the tidal zone, in saline waters containing gram per liter quantities of sulfate (SO_4^{2-}). DSH is a fresh water harbor with milligram per liter concentrations of sulfate. Corrosion in DSH is localized to the top 3 m below the surface and water depth is not significantly influenced by tides.

Table 1 summarizes observations and measurements made in DSH prior to this investigation.[13] The Larson-Skold Index (LSI) that describes the corrosiveness of water toward mild steel is based upon evaluation of in situ corrosion of mild steel lines transporting Great Lakes waters. The index is the ratio of equivalents per million (epm) of SO_4^{2-} and chloride (Cl^-) to the epm of alkalinity in the form bicarbonate plus carbonate. An LSI << 0.8 indicates that Cl^- and SO_4^{2-} probably will not interfere with natural film formation. The LSI for the St. Louis River ranges from 0.22 to 0.65, indicating low corrosiveness. Bushman and Phutt[14] determined that stray currents were not the cause of corrosion in DSH. The corrosion was also determined to be independent of the type and age of the CS. Field and laboratory tests described in this paper were designed to examine the potential role of microorganisms in the localized corrosion.

METHODS AND MATERIALS

Field Experiments

To assess rates of corrosion throughout the harbor, the Duluth Seaway Port Authority (Duluth, Minnesota) and the U.S. Army Corps of Engineers, Detroit District (Detroit, Michigan), developed a system to evaluate the impacts of corrosion on steel of a known mass and over a specific exposure period. A standard coupon consisted of a section of 0.9525-cm-thick A328 (0.035% max. P, 0.04% max. S, and 0.20% min. Cu) cold-rolled sheet pile cut to an average size of 19.3 cm by 11.6 cm and sandblasted to SP5 white metal blast cleaning specification.[15] Prior to exposure, the steel sheet pile structures were washed with a 4,000-psi pressure washer to remove marine growth and any existing corrosion.[16] Sample trays were welded to the clean steel structures (AMI Consulting Engineers, Duluth, Minnesota) using underwater welding techniques as described in American Welding Society specification D3.6[17] using E70XX welding rods. Trays were installed with the top of the tray at 1 m below the Lake Superior International Great Lakes Datum water level.[18] Divers collected coupons from the following locations in the

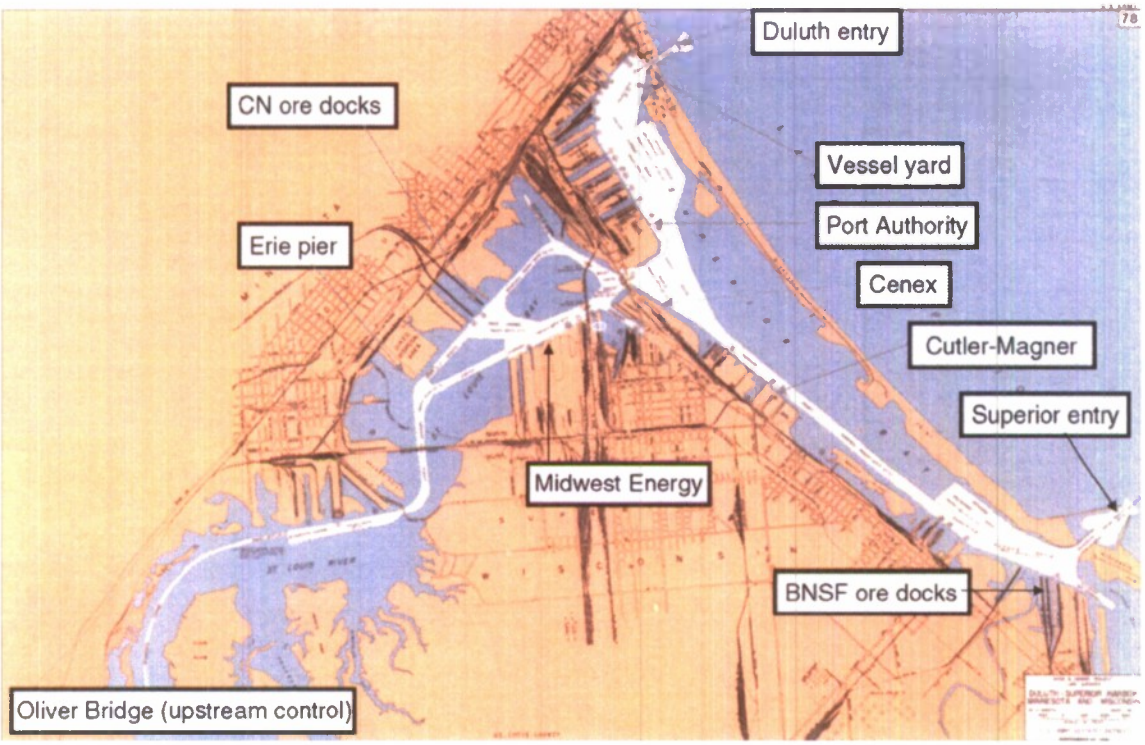

FIGURE 2. *Map of Duluth Superior Harbor, Minnesota and Wisconsin.*

DSH: Cutler-Magner (10/03/06 to 10/08/08 exposure) and Midwest Energy (10/17/06 to 10/08/08 exposure) and upstream in the St. Louis River at Oliver Bridge (10/04/06 to 10/08/08 exposure) (Figure 2). Samples were placed into acrylic boxes with St. Louis River water and shipped to Naval Research Laboratory, Stennis Space Center, Mississippi. Tubercles were intact and covered with water on receipt. Each coupon was removed from its acrylic box and imaged using a digital camera. Tubercles from each coupon were imaged using the macro feature of the digital camera. Select tubercles were embedded in resin epoxy and sectioned using a diamond blade, slow speed saw. The cross sections were imaged with the digital camera. Coupons were fixed in 4% glutaraldehyde ($C_5H_8O_2$) buffered with 0.1 M sodium cacodylate ($[CH_3]_2AsNaO_2 \cdot 3H_2O$) (pH 7.2) and stored overnight in a refrigerator at 4°C. Tubercles were removed with a scalpel and forceps and rinsed in distilled water for 3 min to remove the fixative. Tubercles were used for the following analyses: (1) environmental scanning electron microscopy (ESEM) coupled with energy-dispersive x-ray spectrometry (EDS); (2) transmission electron microscopy (TEM); x-ray diffraction (XRD) and total organic carbon (TOC). Weight-loss and pit depth measurements were used to evaluate corrosion.

Coupons were cleaned according to ASTM G1[19] by washing with a solution of hydrochloric acid (HCl) and distilled water (1:1) with 3.5 g/L of hexamethylene-tetramine ($[CH_2]_6N_4$). Coupons were digitally imaged after cleaning. Pit depths were measured in three locations on each coupon surface with a non-contact optical profiler with a 3.5-mm optical laser pen and averaged. Coupons were weighed to the nearest tenth of a gram before exposure and after acid cleaning.

Tubercles were mounted on a Peltier cooling stage maintained at 4°C in an ESEM. The ESEM was operated at an accelerating voltage of 20 keV with the chamber water vapor pressure between 4 torr and 6 torr. After imaging, the mounted tubercles were examined using EDS. Representative elemental composition spectra and maps of metal surfaces, corrosion products, and surface films were collected.

For examination by TEM, tubercles were removed from the coupons and fixed overnight in 0.1 M sodium cacodylate buffer (pH 7.0), 2.0% formaldehyde (CH_2O), and 2.5% glutaraldehyde; rinsed with distilled water and postfixed 45 min in cacodylate buffered (pH 7.0) 1% osmium tetroxide (OsO_4); dehydrated with an ethanol (C_2H_6O) series (50, 70, 85, 95, and 100%) followed by acetone (CH_3COCH_3); infiltrated in 50/50% by volume resin (nonenyl succinic anhydride [$C_{13}H_{20}O_3$; 26 g], vinyl cyclohexene dioxide [$C_8H_{12}O_2$; 10 g], diglycidyl ether [$C_6H_{10}O_3$; 6 g]), and dimethylaminoethanol ($C_4H_{11}NO$; 0.2 g); and cured at 70°C for 36 h. Ultrathin sections (~90 nm) were taken with a microtome and a diamond knife and collected on 200-mesh Cu grids. Grids were stained with lead citrate ($C_{12}H_{10}O_{14}Pb_3$) and 2% aqueous uranyl acetate ($C_4H_8O_6U$) and viewed using TEM.

Corrosion products in tubercles and from adjacent areas were prepared for XRD with an agate mortar and pestle under nitrogen (N_2), using acetone to prepare a slurry that was transferred to 2.5-cm-diameter glass disks. An x-ray diffractometer was used in the study. The instrument was operated at a voltage of 35 kV and 15 mA current. A step scan from 2° to 70° (2q)θ was used, 0.05° increment and 8 s dwell time per step. A steady stream of N_2 was used to flood the interior of the instrument to prevent oxidation. Data were retrieved and converted to spreadsheets.

TOC analysis of the tubercles was determined using EPA method 415.2.[20] Bonner Analytical Laboratory (Hattiesburg, Mississippi) performed the analyses.

Laboratory Testing

Electrochemical experiments were designed to represent the following sequential conditions on the surface of the pilings:

- —establishment of localized O_2 concentration cells as a result of tubercle formation
- —deposition of Cu under anaerobic conditions
- —formation of a galvanic couple between deposited Cu and underlying CS
- —exposure of the galvanic couple to O_2 when the ice scour disrupts the tubercle

CS (chemical composition by %: 0.17 to 0.23 C, 0.3 to 0.6 Mn, 0.04 P max., 0.05 S max., and balance Fe)[21] was machined into discs 1.58 cm (5/8 in) diameter by 0.158 cm (1/16 in) thickness and squares 10.2 by 10.2 by 0.32 cm (4 by 4 by 1/8 in). Prior to exposure to synthetic lake water, coupons were rinsed in acetone, ethanol, and distilled water and dried with N_2 to removed grease and residual surface debris.

Synthetic lake water (20 ppm or 5.6×10^{-4} M sodium chloride [NaCl]) containing concentrations of 32, 16, 8, and 0 ppm Cu^{2+} (molar concentrations of 5×10^{-4} M, 2.5×10^{-4} M, 1.25×10^{-4} M, and 0 M, respectively) was prepared from deionized water and reagent-grade crystalline copper sulfate pentahydrate ($CuSO_4 \cdot 5H_2O$). To examine the effect of [Cl^-], a solution of 10 ppm Cl^- (2.8×10^{-4} M NaCl) with 32 ppm Cu^{2+} was also prepared. [Cu^{2+}] and [Cl^-] were representative of DSH water (Table 1).[13] There are no data for storm events when the concentrations of Cu could be temporarily higher.

Disc-shaped CS coupons were mounted separately in electrode holders with a knife-edged polytetrafluorothylene (PTFE) gasket defining an exposure area of 1 cm^2. The electrode holder fits into the top of a spherical glass corrosion cell, similar to the standard cell detailed in ASTM G5.[22] A separate 2-L beaker contained one square CS coupon along with a saturated calomel electrode (SCE). New coupons were used for each experiment. A salt bridge was fabricated from plastic tubing filled with saturated potassium chloride (KCl) solution and sealed with glass frits on either end in each of the two containers. At the onset of each experiment, the electrode holder was removed from the corrosion cell, 700 mL of synthetic lake water was added to the corrosion cell and deaerated with dry N_2 for 1 h. At the same time, 500 mL of the same solution was added to the 2-L beaker so that 100 cm^2 of the square CS coupons was submerged. The beaker was left open to air. After 1 h, the electrode holder was placed into the spherical cell so that the entire exposed surface (1 cm^2) of the coupon was submerged in the deaerated solution. The solution was bubbled continually with N_2. The cells were then immediately connected to a computer-controlled potentiostat/zero-resistance ammeter (ZRA)[23] where the 1-cm^2 disc coupon was connected to working electrode (WE) cable, the 100-cm^2 square coupons to the counter electrode (CE) cable, and the SCE to the reference electrode (RE) cable. The two CS coupons were coupled through the ZRA and maintained at the same potential—their couple potential vs. SCE. The current flowing between the two electrodes was recorded every minute over a 24-h period. In this configuration the 1-cm^2 electrode in the deaerated synthetic lake water represents the anaerobic area under the tubercle and the larger electrode represents the surrounding area exposed to O_2. Positive current indicates electrons flowing from the small disc coupon (anode) to the large square coupon (cathode).

After 24 h, the bubbling N_2 was stopped and the cell was opened to air. Galvanic current was measured over the next 24 h. This configuration approximated the condition of the piling surface after ice scour disrupted the tubercles and the Cu-coated CS surface was exposed to aerated water. After the 48-h exposure period (24 h deaerated and 24 h aerated) coupons were removed and corrosion morphology was examined using ESEM. In a separate series of experiments, electrodes were removed after the 24-h deaeration, and the approximate concentration of surface-bound Cu was determined using ESEM/EDS.

In addition, anodic potentiodynamic scans were performed on two 1-cm^2 CS coupons after a 24-h deaerated exposure (coupled to separate 100-cm^2 CS cathodes) to two different solutions: (1) 32 ppm Cu^{2+}/20 ppm Cl^- and (2) 0 ppm Cu^{2+}/20 ppm Cl^-. After 24 h, the coupons were left in the corrosion cell but the couple was disconnected from the 100-cm^2 coupon. While maintaining deaerated conditions by bubbling N_2, a graphite rod and a SCE were inserted into the corrosion cell for use as counter and reference electrodes, respectively. Potentiodynamic scans were performed using the same computer-controlled potentiostat/ZRA as described previously. Scans were started at a potential –0.005 V relative to a 1-h stabilized corrosion potential to 0.2 V_{SCE} at a scan rate of 1 mV/s. This scan rate was chosen over the conventional 0.167-mV/s scan rate[22] to reduce the total scan time, thus decreasing dissolution of the coupon and alteration of the surface-bound Cu.

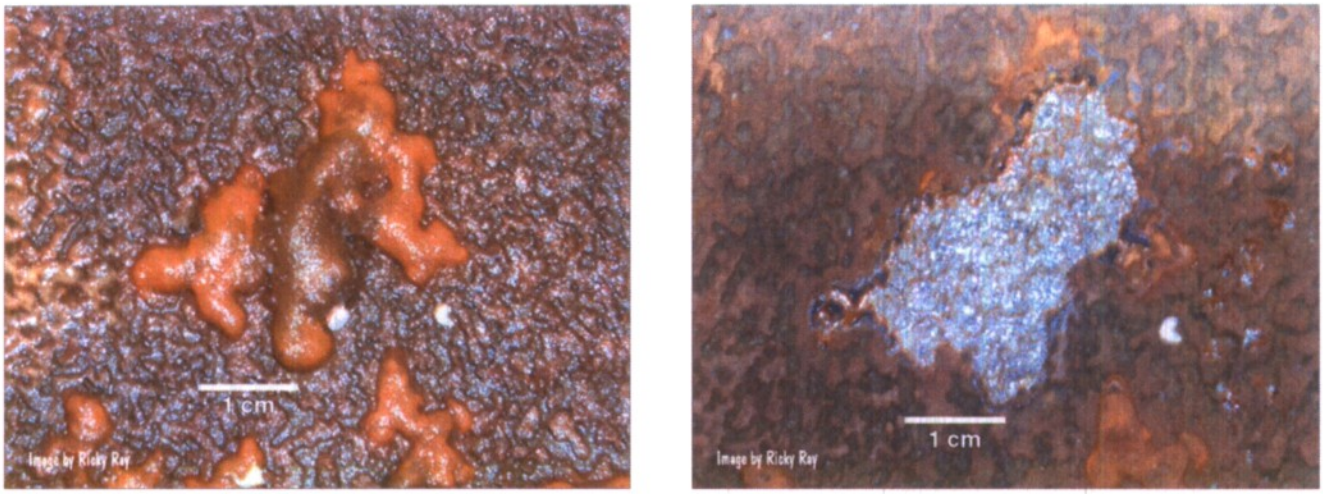

(a) (b)

FIGURE 3. *(a) Image of tubercle on CS surface and (b) after physical removal of tubercle exposing pits underneath the tubercle.*

RESULTS

Field Experiments

All coupons recovered from DSH were covered with tubercles (Figure 3[a]). Pits were exposed when tubercles were removed (Figure 3[b]). Tubercles were distributed randomly on both sides of the coupons. XRD data indicated that tubercles from all three locations were amorphous Fe oxides surrounded by magnetite. TEM micrographs confirmed amorphous Fe oxides in association with bacteria (Figure 4). All tubercles were made up of porous layers or strata. Diatoms, animals with siliceous frustules, colonized the topsides of the tubercles, and an EDS spectrum of the topside indicated the presence of Mg, Al, Si, S, K, Ca, and Mn in addition to Fe. The underside of the tubercle, the surface that had been in contact with the metal, was comprised of bacteria with two predominant morphologies: large rod-shaped bacteria (Figure 5[a]) and long Fe-encrusted filaments (Figure 5[b]). The underside of the tubercle contained elevated concentrations of S, Sn, Cr, and Cu compared to the exterior. A digital image of a cross section through a tubercle (Figure 6[a]) illustrates the layered morphology of a DSH tubercle. Cu is evident as a greenish sheen in a digital image of a planar view of the underside of a tubercle (Figure 6[b]). An ESEM micrograph (Figure 6[c]) and the corresponding EDS dot map (Figure 6[d]) of the surface of the tubercle that had been in contact with the metal illustrate the uniform distribution of Cu under the tubercle. Average pit depth, weight loss, and TOC data for the three locations are summarized in Table 2. Averaged pit depth ranged from 538 μm ± 65.8 to 398 μm ± 27.1; weight loss, from 60.5 g to 41.7 g; and TOC, from 33.9 mg/kg to 22.6 mg/kg.

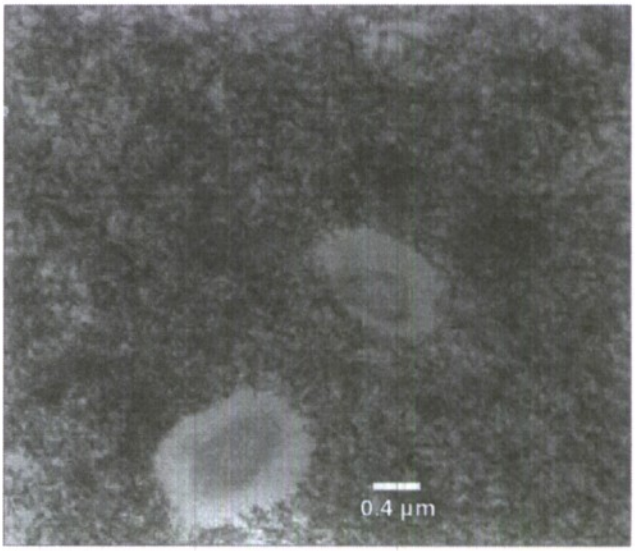

FIGURE 4. *TEM micrograph of tubercle interior in cross section, showing two bacteria (1.2 μm diameter) surrounded with amorphous iron oxides.*

Laboratory Experiments

In all cases CS surfaces exposed in deaerated solutions spiked with Cu^{2+} were covered with Cu within a few hours as demonstrated by a dark orange surface, while exposure to the unspiked solution remained a dull gray. Figure 7 shows the galvanic current (μA) vs. time (h) traces for 1-cm^2 CS coupons in deaerated solutions of varying [Cu^{2+}] coupled to 100-cm^2 CS coupons in the same solution under aerated conditions. A [Cl^-] of 20 ppm was maintained in all solutions. The data trace for the 32-ppm Cu^{2+} solution indicates a peak positive current of 15.0 μA after 1 h, with a steady decrease to 7.5 μA after 24 h. The

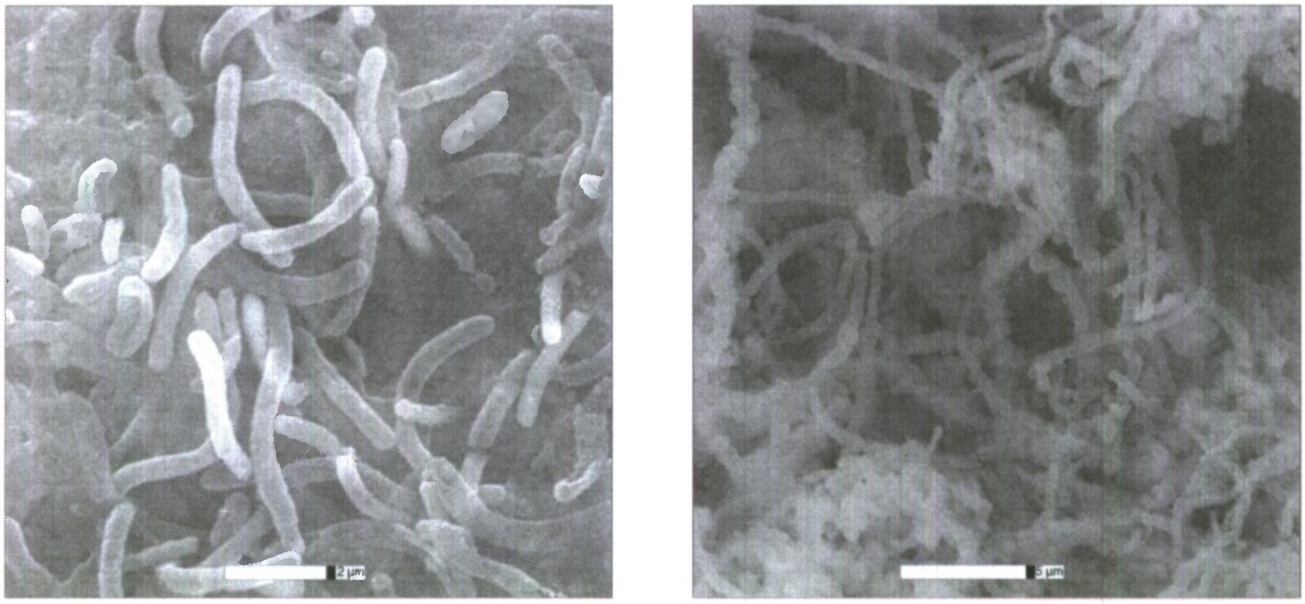

(a) (b)

FIGURE 5. *ESEM micrographs from the underside of a tubercle indicating the presence of (a) large rod-shaped bacteria and (b) long iron-encrusted filaments.*

16-ppm Cu^{2+} solution shows the same trend as the 32-ppm case but with a smaller peak of 8.5 µA (at 3 h) with a steady decrease to 6.0 µA after 24 h. In contrast, the 8-ppm Cu^{2+} solution does not show a definitive peak, instead the current sharply rises from –1.7 µA to 1.9 µA after 1 h. The current continues to increase to a value of 3.2 µA after 24 h. For the 0-ppm Cu^{2+} solution, initial current is –6.4 µA and increases (less negative) to –0.8 µA after 2 h. Current slowly increases to –0.2 µA but does not become positive after 24 h, unlike the experiments with Cu^{2+} in solution. When the peak current value (µA) for each solution is plotted vs. the ppm $[Cu^{2+}]$ in solution, a positive linear trend is observed (Figure 8).

Figure 9 shows the galvanic current (µA) vs. time (h) traces of the couples after the deaerated solutions were open to air. Initially, all current profiles were negative for solutions spiked with Cu^{2+}. The solution with 32 ppm Cu^{2+} had the most negative value of –19.3 µA. After 0.5 h, these current traces increased to positive values. Currents for the 32-ppm and 16-ppm Cu^{2+} solutions continued to increase throughout the 24-h period, while current for the 8-ppm solution showed a decrease after the initial peak. In contrast to the Cu-containing solutions, the 0-ppm Cu^{2+} solution had an initial current which was positive (5.3 µA) and then decreased to 2.5 µA in the first hour. The current increased to 3.3 µA after 3 h and then slowly decreased to 2.5 µA for the remainder of the 24-h exposure period. When the peak current value for each solution is plotted vs. the ppm Cu^{2+} concentration in solution, a positive linear trend is only observed through non-zero values of $[Cu^{2+}]$ (Figure 10). Currents for the 32-ppm and 16-ppm cases continued to increase at the end of the exposure; therefore, the peak current may not have been reached during the 24-h period.

The effects of varying $[Cl^-]$ from 20 ppm to 10 ppm at a constant $[Cu^{2+}]$ of 32 ppm for both the deaerated and aerated exposures are illustrated in Figures 11 and 12, respectively. For the deaerated exposure (Figure 11), similar curve trends are observed for the two different $[Cl^-]$. The 10-ppm Cl^- solution has a slightly smaller peak current of 13.9 µA (vs. 15.0 µA for 20 ppm Cl^-) with both solutions showing a current decrease to ~8.0 µA after 24 h. For the aerated exposure (Figure 12), the current trends are again similar, except the lower $[Cl^-]$ slowly decreases after peaking at 6.2 µA after 1.5 h in contrast to the 20-ppm $[Cl^-]$ solution, which continues to increase.

Anodic potentiodynamic scans performed on deaerated 1-cm^2 CS coupons are shown in Figure 13 after 24 h of deaerated exposure and coupling to the 100-cm^2 aerated coupon. Exposure to 32 ppm Cu^{2+} and 0 ppm Cu^{2+} (both with 20 ppm Cl^-) had similar corrosion potentials of –0.682 V_{SCE} and –0.653 V_{SCE}, respectively. Anodic scans of the 32-ppm Cu^{2+} exposure produced current values an order-of-magnitude higher than the exposure with 0 ppm Cu^{2+}.

The surface Cu concentration of each 1-cm^2 CS coupon (coupled to the 100-cm^2 coupon) after 24 h of deaerated exposure was determined semi-quantitatively using EDS for each Cu^{2+} solution. A 50-wt% Cu surface concentration was measured after exposure to the 32-ppm Cu^{2+} solution, with the balance being Fe. Cu concentrations of 21% and 20% were measured for

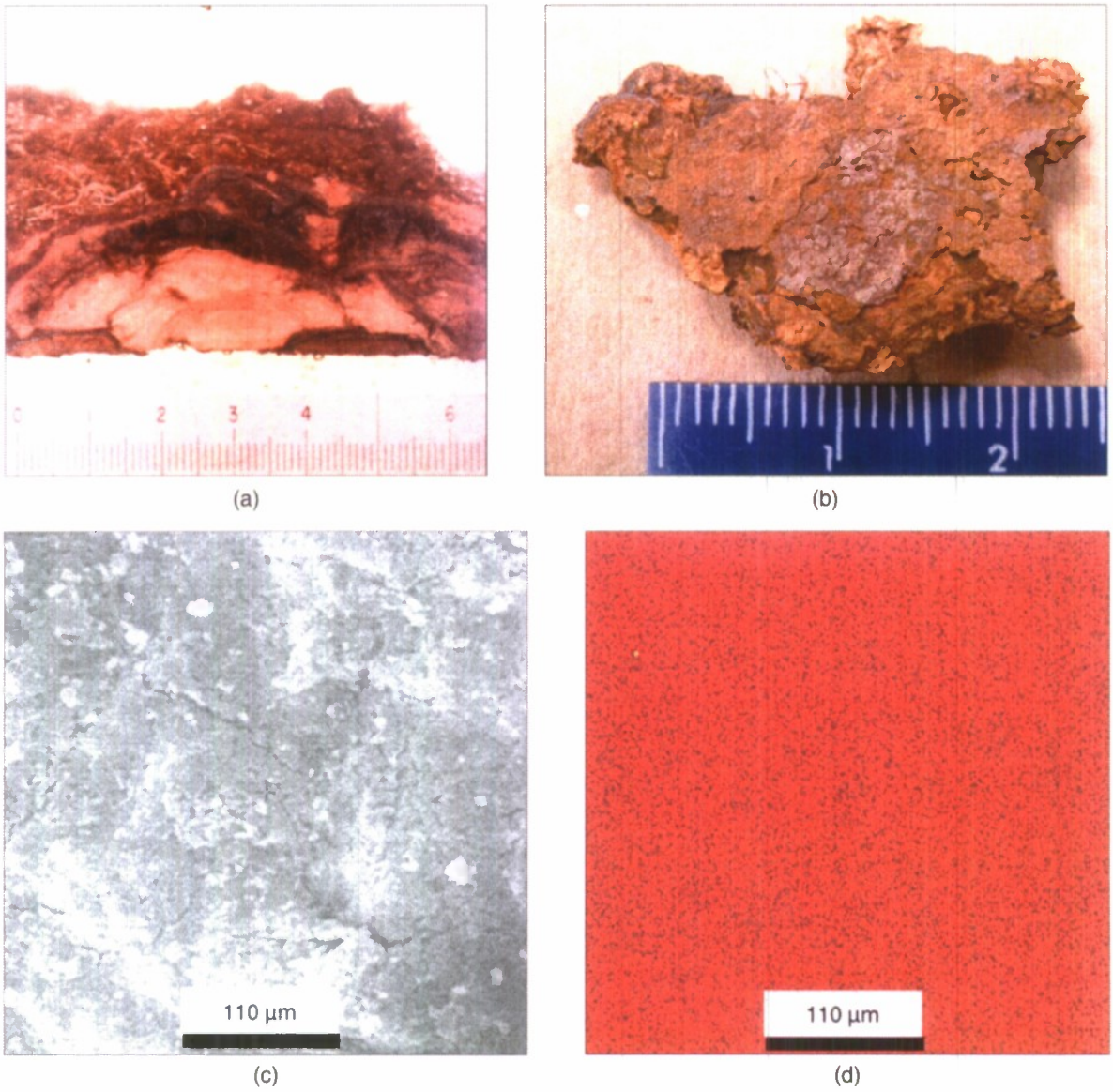

FIGURE 6. *(a) Cross section of resin-embedded DSH tubercle, showing layers of material within the core. The scale bar indicates 0 to 0.6 mm. (b) Planar view of the underside of a tubercle. Green sheen is due to accumulation of Cu. (c) ESEM micrograph and (d) corresponding EDS dot map illustrate the homogeneity of Cu layer that had been in contact with the CS surface under the tubercle.*

exposures to the 16-ppm and 8-ppm Cu^{2+} solutions, respectively. No Cu was measured on the coupon surface exposed to the 0-ppm Cu^{2+} solution.

After the 48-h exposure period (24 h deaerated and 24 h aerated) coupons were removed and corrosion morphology was documented using ESEM. Presence of Cu^{2+} in solution resulted in small (25 µm to 75 µm diameter) pits on CS surfaces. No pits were observed in the absence of Cu.

DISCUSSION

CS panels from three locations, two inside DSH (i.e., Cutler-Magner and Midwest Energy) and upstream of the DSH (i.e., Oliver Bridge), were similar in the following characteristics:

—Tubercles formed on both sides of the coupons.
—Tubercles were composed of amorphous Fe oxides associated with bacteria.
—Tubercle surfaces were colonized with diatoms.
—Tubercles were made up of chemically distinct strata.
—The innermost stratum of tubercles contained heavy metals including Cr, Mn, and Ni with a distinct layer of Cu (Figure 6).

Tubercles located on both sides of the coupons indicated that their formation was not influenced by light. Weight loss, a measurement of general or uniform

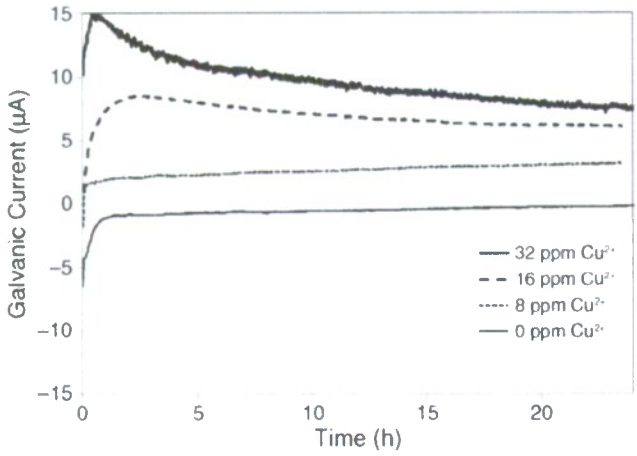

FIGURE 7. *Galvanic current (μA) measured for 24 h for the 1-cm² CS coupon in deaerated solutions with 20 ppm Cl⁻ and different [Cu²⁺] coupled to the 100-cm² CS coupon exposed to the same solution under aerated conditions.*

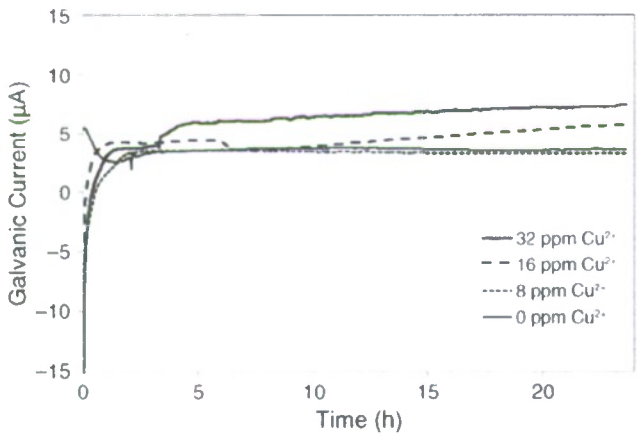

FIGURE 9. *Galvanic current (μA) measured for 24 h after deaerated solutions (Figure 7) were opened to air.*

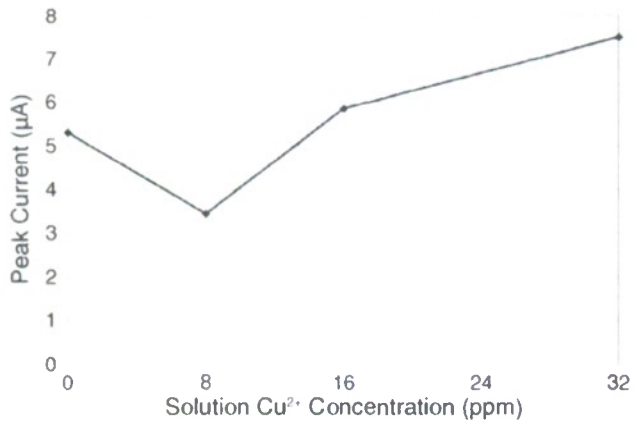

FIGURE 10. *Peak galvanic current (μA) measured during the second 24 h of exposure under aerated conditions (for the 1-cm² coupon) vs. the [Cu²⁺] in solution.*

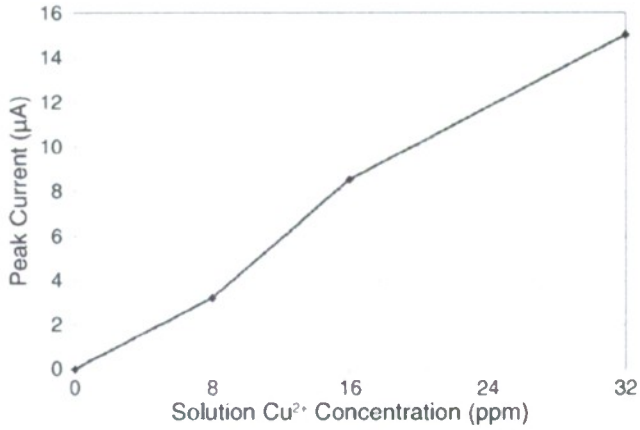

FIGURE 8. *Peak galvanic current (μA) measured during the first 24 h of exposure under deaerated conditions (for the 1-cm² coupon) vs. the [Cu²⁺] in solution.*

corrosion, and pit depth, a measure of localized corrosion, indicated the same trends in corrosion: Cutler-Magner > Midwest Energy > Oliver Bridge (Table 2).

In the present study, we established a spatial relationship between bacteria, tubercles, deposited Cu, and localized corrosion. TEM and ESEM images (Figures 4 and 5) demonstrated bacteria associated with the tubercle interior. Twisted filaments found in the DSH tubercles (Figure 5[b]) are typical of sheath-producing microaerophilic iron-oxidizing bacteria (IOB), e.g., *Gallionella*. The bacterium is a kidney-shaped cell (not evident in Figure 5[b]) with an elongated stalk made up of helically wound mineralized fibrils.[24] Hicks[25] previously isolated an IOB from corroded areas on coupons exposed in DSH and identified the organism as *Sideroxydans lithotrophicus* by sequencing the 16S rDNA. In his studies, the IOB from corroded surfaces could not be isolated from non-corroding surfaces. IOB derive energy from the oxidation of ferrous (Fe^{2+}) to ferric (Fe^{3+}) at near-neutral pH, and in some cases the result is the formation of dense tubercles or rusticles of filamentous Fe oxides. At pH > 5, Fe^{2+} spontaneously oxidizes to Fe^{3+} ($t_{1/2}$ < 15 min). At circumneutral pH, IOB compete with abiotic Fe^{2+} oxidation in low-O_2 environments. Druschel, et al.,[26] determined that the maximum O_2 levels associated with the growth of *Sideroxydans lithotrophicus* were 15 μM to 50 μM. O_2 gradients are produced by biofilms on surfaces.[27] The dissolved O_2 concentration in DSH bulk waters is routinely 7 ppm (219 μM) or greater and does not vary systematically with depth. IOB have been reported in Lake Superior, particularly associated with rusticles on shipwrecks, e.g., *Comet*, *Osborne*, and *Edmund Fitzgerald*.[28]

MIC is defined as corrosion resulting from the presence and/or activities of microorganisms.[29] IOB have been implicated in MIC since the 1960s.[30] It is well established that tubercle formation by IOB pro-

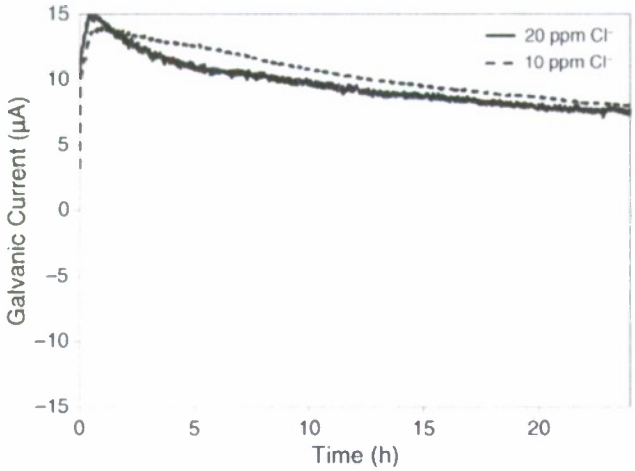

FIGURE 11. *Galvanic current (μA) measured for 24 h for the 1-cm² CS coupon in deaerated solutions of 10 ppm and 20 ppm Cl^- with 32 ppm Cu^{2+} coupled to the 100-cm² CS coupon exposed to the same solution under aerated conditions.*

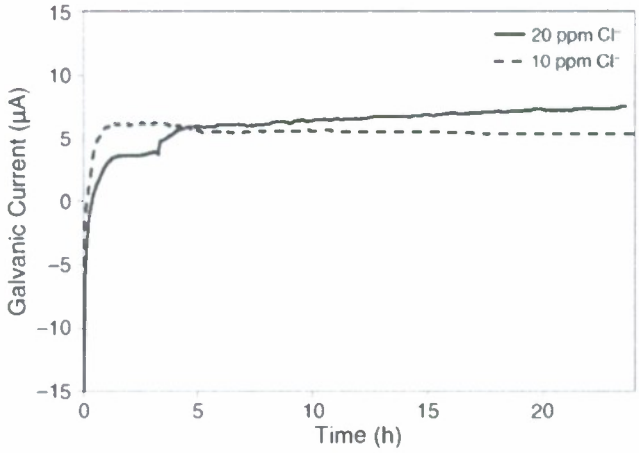

FIGURE 12. *Galvanic current (μA) measured for 24 h after deaerated solutions (Figure 11) of 10 ppm and 20 ppm Cl^- with 32 ppm Cu^{2+} were opened to air.*

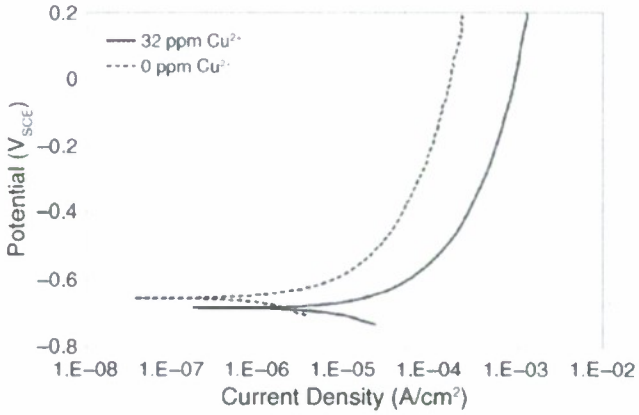

FIGURE 13. *Anodic polarization scans of the 1-cm² CS coupons after 24 h exposure in deaerated solutions of 32 ppm and 0 ppm Cu^{2+} with 20 ppm Cl^-.*

duces an O_2 concentration cell. Most of the documented MIC case histories associated with IOB tubercle formation have involved exposure of austenitic 300 series (Types 304 [UNS S30400] or 316 [UNS S31600][11]) stainless steels in untreated well water (200 ppm to 300 ppm [Cl^-]) and chlorinated drinking water.[31-39] IOB form dense deposits, excluding O_2 from the area immediately under the deposit. In an oxygenated environment, the area deprived of O_2 becomes a relatively small anode compared to the large surrounding oxygenated cathode. Metal is oxidized at the anode and pH decreases. The extent of the decrease is determined by the alloy composition.[40] For this reason, O_2 concentration cells produce particularly aggressive corrosion on 300 series stainless steels, containing 17.5% to 20% Cr. Cl^- migrates from the electrolyte to the anode to neutralize charge, forming heavy metal chlorides that are extremely corrosive. Under these circumstances, pitting involves the conventional features of differential aeration, a large cathode:anode surface area, and the development of acidity and metallic chlorides.

Corrosion of CS in DSH cannot be due to the well-characterized mechanism for IOB-influenced corrosion of 300 series stainless steels. The electrochemical experiments described in this paper confirm that differential aeration cells alone do not cause aggressive corrosion of CS in fresh water (Figure 7, 0 ppm Cu^{+2}). Furthermore, varying [Cl^-] did not greatly impact the galvanic current behavior in the presence of 32 ppm Cu^{2+} under any test condition (Figures 11 and 12).

Accelerated corrosion of CS in contact with Cu in fresh water has been acknowledged since the early 1920s.[41] In our studies, Cu^{2+} precipitated on anaerobic CS surfaces (Figures 6[b] through [d]). A positive current established by the galvanic couple between the Cu-coated CS (anaerobic anode) and the larger CS (aerobic cathode) was initially high, but stabilized within a few hours (Figure 7). The positive value of the galvanic current indicated that the anode was preferentially corroding with respect to the cathode. Peak positive galvanic current scaled linearly with solution

TABLE 2
Average Pit Depth, Weight Loss, and Total Organic Carbon Data for the Three Locations at Duluth Superior Harbor, Minnesota and Wisconsin

	Cutler-Magner	Midwest Energy	Oliver Bridge
Average pit depth (μm)	538 ± 65.8	482 ± 81.0	398 ± 27.1
Weight loss (g)	60.5	44.4	41.7
Total organic carbon (mg/kg)	33.9	22.6	33.2

[11] UNS numbers are listed in *Metals and Alloys in the Unified Numbering System*, published by the Society of Automotive Engineers (SAE International) and cosponsored by ASTM International.

[Cu^{2+}] (Figure 8) and can be explained by increased anodic kinetics for Cu-coated CS under anaerobic conditions (Figure 13). When O_2 was introduced to the anaerobic anode, the galvanic current decreased to negative values for all solutions spiked with Cu^{2+} (Figure 9). With both coupons exposed to O_2, the Cu-coated CS coupon had a higher corrosion potential than the larger CS coupon due to Cu having a higher redox potential than Fe. However, after 0.5 h the galvanic current increased to positive values, indicating that the Cu-coated coupon was again preferentially corroding with respect to the larger CS coupon. Ice scouring breaks tubercles, which allows ingress of O_2 and aggressive corrosion. The depth of the aggressive corrosion coincides with the range over which ice scour is reportedly important. The peak galvanic current under both anaerobic and aerobic conditions is related to [Cu^{+2}] over the range from 0 to 32 ppm (Figures 8 and 10).

Several investigators have reported metal-binding, including Cu, by bacterial exopolymers.[42-43] Others have demonstrated that bacterial EPS rich in uronic acids promote deterioration of metals.[44-45] Geesy, et al.,[46] described deterioration of a metallic Cu film due to the formation of Cu concentration cells. In their studies, cells of an adherent freshwater bacterium produced exopolymers capable of binding Cu^{+2}, creating Cu concentration gradients on the surface.

Bacteriogenic Fe oxides, made up of intact and/or partly degraded remains of bacterial cells mixed with amorphous hydrous ferric oxides, are formed in response to chemical or bacterial oxidation of Fe^{2+} to Fe^{3+}.[47] Bacteriogenic Fe oxides have reactive surfaces and act as sorbents of dissolved metal ions, and enrichments of Pb, Cd, Al, Cu, Cr, Mn, Sr, and Zn have been reported.[48-49] The TOC in the DSH tubercles, ranging from 22.6 mg/kg to 33.9 mg/kg, demonstrated an organic component in the corrosion products. Gerke, et al.,[50] examined five tubercles from a single drinking water distribution system, evaluating morphology, mineralogy, and chemistry. The overall morphology of all five samples was similar—a core (either soft or hard) with a hard shell layer covered with surface material. They demonstrated that heavy metals were either trapped within the structure or sorbed onto regions of the tubercles. The overall morphology of DSH tubercles was similar to that described by Gerke, et al.[50] The possibility that bacteriogenic Fe oxides in DSH tubercles sorbed Cu was considered and discarded. The distribution of Cu in the DSH tubercles was a well-defined layer at the base of the tubercles (Figures 6[b] through [d]).

The individual events leading to the corrosion of CS pilings in DSH are predictable, i.e., colonization of the surface by IOB followed by the establishment of differential aeration cells. However, this is the first report of deposition of Cu as a result of microorganisms and the influence on corrosion of CS.

CONCLUSIONS

❖ A combination of biological, chemical, and physical events contribute to the corrosion of CS pilings in DSH. Dense deposits of IOB create conditions for Cu precipitation on CS surfaces. Ice scouring disrupts the tubercles and exposes localized areas of Cu-covered CS to O_2. The resulting galvanic cell produces aggressive localized corrosion. The individual events in the sequence are predictable, but have not been previously reported. No attempt has been made to relate the galvanic current measurements made in the laboratory to the corrosion measured in the field. Galvanic current is related to the aggressiveness of the corrosion but cannot be converted to corrosion current or rate of penetration. In our experiments the magnitude of the galvanic current is related to the amount of Cu deposited on the surface, which is directly related to the concentration of dissolved Cu^{2+}. The magnitude of the galvanic current measured in the laboratory will also be related to the anode:cathode area ratios. We have no information about these relative areas on the pilings.

ACKNOWLEDGMENTS

This work was supported by the U.S. Army Corps of Engineers, Detroit District, Duluth Seaway Port Authority, and NRL 6.1 Program Element number 0601153N. XRD data were collected by A. Falster, MicroBeam Laboratory in the Department of Geology and Geophysics at the University of New Orleans, New Orleans, Louisiana. TEM images were obtained by K. Curry, Department of Biological Sciences at the University of Southern Mississippi, Hattiesburg, Mississippi. NRL Publication number JA 7330/09/9285.

REFERENCES

1. ASTM A328/A328M-07, "Standard Specification for Steel Sheet Piling" (West Conshohocken, PA: ASTM International, 2007).
2. R. Mitman, *Mater. Perform.* 45, 5 (2006): p. 16-19.
3. K.R. Larsen, *Mater. Perform.* 47, 10 (2008): p. 22-26.
4. C.A. Wortley, *Great Lakes Small Craft Harbor and Structure Design for Ice Conditions: An Engineering Manual* (Madison, WI: University of Wisconsin Sea Grant Institute, 1985).
5. W.C. Kerfoot, S. Hartting, R. Rossmann, J.A. Robbins, *J. Great Lakes Res.* 25, 4 (1999): p. 663-682.
6. W.C. Kerfoot, J.A. Robbins, *J. Great Lakes Res.* 25, 4 (1999): p. 697-720.
7. M. Sydor, *J. Geophys. Res.* 83, C8 (1978): p. 4,074-4,078.
8. C.W. Scott, G. Clark, J. Radniecki, "Accelerated Fresh Water Corrosion Study and Remediation of Steel Structures," Cold Region Engineering 2009: Cold Regions Impacts on Research, Design, and Construction (Reston, VA: American Society of Civil Engineers, 2009), p. 627-636.
9. D. Johnson, J.M. Moulin, R. Karius, B. Reslak, M. Confete, W.T. Chao, "Low Water Corrosion on Steel Piles in Marine Waters," Final Report, EUR 17868, 1994.
10. I.B. Beech, S.A. Campbell, *Electrochim Acta* 54 (2008): p. 14-21.
11. R.B. Oubner, I. Beech, "Statistical Assessment of the Risk of the Accelerated Low-Water Corrosion in the Marine Environment," CORROSION/99, paper no. 99318 (Houston, TX: NACE International, 1999).
12. T. Gehrke, W. Sand, "Interactions Between Microorganisms and Physicochemical Factors Cause MIC of Steel Pilings in Harbours

(ALWC)," CORROSION/2003, paper no. 03557 (Houston, TX: NACE, 2003).
13. "Minnesota Milestone River Monitoring Program—Lake Superior Basin," Minnesota Pollution Control Agency, March 26, 2007, http://www.pca.state.mn.us/water/milestone-sites.html#superior, June 29, 2009
14. J.B. Bushman, B.S. Phull, "High Voltage Direct Current (HVDC) Interference Determination for Duluth Superior Harbor," Report to NTH/WTA Joint Venture, December, 2008.
15. SSPC-SP 5/NACE No. 1, "White Metal Blast Cleaning" (Houston, TX: NACE, 2006).
16. SSPC-SP 7/NACE No. 4, "Joint Surface Preparation Standard: Brush-Off Blast Cleaning" (Houston, TX: NACE, 2006).
17. AWS Standard D3.6M, "Specification for Underwater Welding" (Miami, FL: American Welding Society, 1999).
18. "IGLD 1985 Brochure on the International Great Lakes Datum 1985," Coordinating Committee on Great Lakes Basic Hydraulic and Hydrologic Data, 1992, http://huron/lrc/usace.army.mil/IGLD.1985/igldmpg.html, June 1, 2009.
19. ASTM G1-03, "Standard Practice for Preparing, Cleaning, and Evaluating Corrosion Test Specimens (West Conshohocken, PA: ASTM International, 2003).
20. EPA Method 415.2, "Total Organic Carbon in Water" (Washington, DC: Environmental Protection Agency, 1999).
21. J.R. Davis, ed., *Metals Handbook, 2nd ed.* (Materials Park, OH: ASM International, 1998).
22. ASTM G5-94, "Standard Reference Test Method for Making Potentiostatic and Potentiodynamic Anodic Polarization Measurement (West Conshohocken, PA: ASTM International, 2004).
23. S.M. Gerchakov, B.J. Little, P.A. Wagner, *Corrosion* 42, 11 (1986): p. 689-692.
24. H.F. Ridgeway, E.G. Means, B.H. Olson, *Appl. Environ. Microbiol.* 41, 4 (1981): p. 288-297.
25. R.E. Hicks, "Structure of Bacterial Communities Associated with Accelerated Corrosive Loss of Port Transportation Infrastructure," Final Report, Nov. 21, 2007.
26. G.K. Druschel, D. Emerson, R. Sutka, P. Suchecki, G.W. Luther, *Geochim. Cosmochim. Acta* 72 (2008): p. 3,358-3,370.
27. Z. Lewandowski, H. Beyenal, *Fundamentals of Biofilm Research* (Boca Raton, FL: CRC Press, 2007).
28. B.J. Little, J.S. Lee, "Microbiologically Influenced Corrosion," in *Kirk-Othmer Encyclopedia of Chemical Technology* (Hoboken, NJ: John Wiley & Sons, Inc., 2009), p. 1-38.
29. B.J. Little, J.S. Lee, *Microbiologically Influenced Corrosion* (Hoboken, NJ: John Wiley and Sons, Inc., 2007).
30. J.M. Sharpley, *Corrosion* 17, 8 (1961): p. 92-96.
31. S.W. Borenstein, P.B. Lindsay, *Mater. Perform.* 27, 3 (1988): p. 51-54.
32. J.T. Borenstein, P.B. Lindsay, *Mater. Perform.* 33, 4 (1994): p. 43-45.
33. G. Kobrin, *Mater. Perform.* 15, 7 (1976): p. 38-43.
34. D.H. Pope, R.J. Soracco, E.W. Wilde, *Mater. Perform.* 21, 7 (1982): p. 43-50.
35. D.H. Pope, D.J. Duquette, A.H. Johannes, P.C. Wayner, *Mater. Perform.* 23, 4 (1984): p. 14-18.
36. G. Kobrin, ed., *A Practical Manual on Microbiologically Influenced Corrosion* (Houston, TX: NACE, 1993).
37. P.R. Puckorius, *Mater. Perform.* 22, 12 (1983): p. 19-22.
38. J.G. Stoecker, *Mater. Perform.* 24, 8 (1984): p. 48-56.
39. A.K. Tiller, *Microbial Corrosion* (London, U.K.: The Metals Society, 1983).
40. L.L. Shreir, R.A. Jarman, G.T. Burstein, eds., *Corrosion—Metal/Environment Reactions, 3rd ed.* (London, U.K.: Butterworth-Heinemann Ltd., 1994).
41. W.G. Whitman, R.P. Russell, *Ind. Eng. Chem.* 16, 3 (1924): p. 276-279.
42. T.E. Ford, J.S. Maki, R. Mitchell, "The Role of Metal-Binding Bacterial Exopolymers in Corrosion Processes," CORROSION/87, paper no. 87380 (Houston, TX: NACE, 1987).
43. B.J. Little, P.A. Wagner, P. Angell, D.C. White, *Int. Biodeter. Biodegr.* 37, 3-4 (1996): p. 159-162.
44. I.B. Beech, C.C. Gaylarde, *Int. Biodeter. Biodegr.* 27 (1991): p. 95-107.
45. G.G. Geesey, M.W. Mittleman, "The Role of High-Affinity, Metal-Binding Exopolymers of Adherent Bacteria in Microbial-Enchanced Corrosion," CORROSION/85, paper no. 85297 (Houston, TX: NACE, 1985).
46. G.G. Geesey, M.W. Mittleman, T. Iwaoka, P.R. Griffiths, *Mater. Perform.* 25, 2 (1986): p. 37-40.
47. F.G. Ferris, *Geomicrobiol J.* 22, 3/4 (2005): p. 79-85.
48. D. Dong, X. Hua, Y. Li, J. Zhang, D. Yan, *Environ. Sci. Technol.* 37, 18 (2003): p. 4,106-4,112.
49. R.E. Martinez, F.G. Ferris, *Am. J. Sci.* 305, 6 (2005): p. 854-871.
50. T.L. Gerke, J.B. Maynard, M.R. Schock, D.L. Lytle, *Corros. Sci.* 50 (2008): p. 2,030-2,039.

A new world of research is in your hands

Save valuable research time with searchable indexes of articles appearing in CORROSION *(COR•Lit) and* Materials Performance *(MP•Lit)*

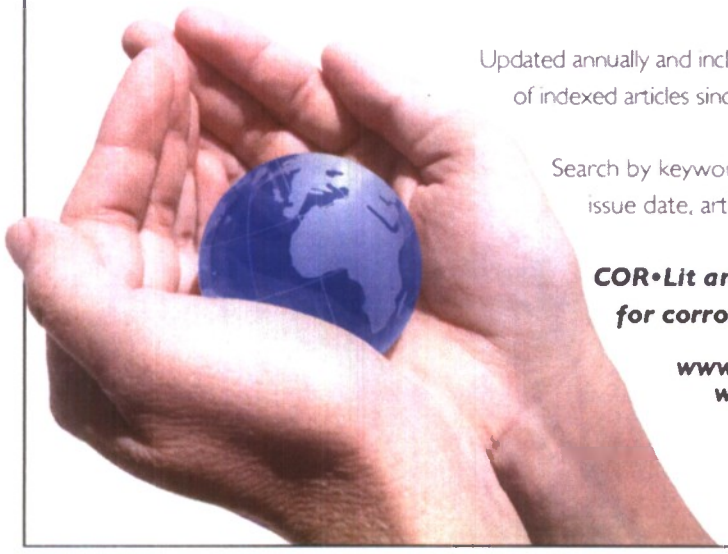

Updated annually and including more than 8,000 articles, COR•Lit provides citations of indexed articles since 1945. MP•Lit references all articles indexed since 1964.

Search by keyword or phrase to generate a list of citations identifying the issue date, article title, author, and page number.

COR•Lit and MP•Lit—your source for corrosion-related abstracts.

www.nace.org/CORLit
www.nace.org/MPLit

NACE INTERNATIONAL
THE CORROSION SOCIETY